Intrastrand Cross-Linked Actin between Gln-41 and Cys-374. III. Inhibition of Motion and Force Generation with Myosin†

Eldar Kim,‡ Elena Bobkova,‡ Carl J. Miller,‡ Albina Orlova,§ György Hegyi,|| Edward H. Egelman,§ Andras Muhlrad,‡,⊥ and Emil Reisler*,‡

Department of Chemistry and Biochemistry and the Molecular Biology Institute, University of California, Los Angeles, California 90095, Department of Cell Biology and Neuroanatomy, University of Minnesota Medical School, Minneapolis, Minnesota 55455, and Department of Biochemistry, Eötvös Lorand University, H-1088 Budapest, Hungary

Received May 29, 1998; Revised Manuscript Received September 24, 1998

ABSTRACT: Structural and functional properties of intrastrand, ANP (*N*-(4-azido-2-nitrophenyl)-putrescine) cross-linked actin filaments, between Gln-41 and Cys-374 on adjacent monomers, were examined for several preparations of such actin. Extensively cross-linked F-actin (with 12% un-cross-linked monomers) lost at 60 °C the ability to activate myosin ATPase at a 100-fold slower rate and unfolded in CD melting experiments at a temperature higher by 11 °C than the un-cross-linked actin. Electron microscopy and image reconstruction of these filaments did not reveal any gross changes in F-actin structure but showed a change in the orientation of subdomain 2 and a decrease in interstrand connectivity. Rigor and weak (in the presence of ATP) myosin subfragment (S1) binding and acto-S1 ATPase did not show major changes upon 50% and 90% ANP cross-linking of F-actin; the K_d and K_m values were little affected by the cross-linking, and the V_{max} decreased by 50% for the extensively cross-linked actin. The cross-linking of actin (50%) decreased the mean speed and the number of sliding filaments in the in vitro motility assays by ∼35% while the relative force, as measured by using external load in these assays, was inhibited by ∼25%. The mean speed of actin filaments decreased with the increase in their cross-linking and approached 0 for the 90% cross-linked actin. Also examined were actin filaments reassembled from cross-linked and purified ANP cross-linked dimers, trimers, and oligomers. All of these filaments had the same acto-S1 ATPase and rigor S1 binding properties but different behavior in the in vitro motility assays. Filaments made of cross-linked dimers moved at ∼50% of the speed of the un-cross-linked actin. The movement of filaments made of cross-linked trimers was inhibited more severely, and the oligomer-made filaments did not move at all. These results show the uncoupling between force generation and other events in actomyosin interactions and emphasize the role of actin filament structure and dynamics in the contractile process.

Much information has been accumulated over the years about the structure and dynamic properties of myosin and its function in the acto-myosin cross-bridge cycle (*1*, *2*). In contrast, the role of F-actin[1] in the cross-bridge cycle has been studied less extensively, perhaps because of the perception that F-actin is a passive element in the force-producing process. This commonly accepted view has been questioned by Oosawa (*3*) who suggested that F-actin participates in the generation of movement during the cross-bridge cycle and that the dynamics and flexibility of the actin filament is an important component of force generation by the acto-myosin system.

As discussed in the preceding publication (*4*), there are several reasons for a closer examination of the role of actin dynamics in the myosin cross-bridge cycle. The flexibility of the filament structure (*5*) is now well-established, and multiple conformational states of F-actin have been related to the presence of a specific metal cation, nucleotide, and phosphate ion (or its analog) in the nucleotide cleft (*6*−*10*). In addition, the internal dynamics and structure of F-actin, including the twist of the filament, can be modified by the interactions with other proteins (*11*). The transitions between the different states of F-actin appear to be mainly associated with changes in the conformation and orientation of subdomain 2 and the actin's C-terminus (*7*, *8*, *10*, *12*). The same sites on actin are influenced strongly by the ligands in the nucleotide cleft in G-actin (*13*) and appear to be coupled to each other intra- and intermolecularly in F-actin (*14*, *15*). Furthermore, the C-terminus and subdomain 2 of actin are proposed to be at the intermolecular interface in F-actin (*16*−*18*) adding to the potential significance of structural changes in this region.

† This work was supported by grants from Hungarian National Research Fund OTKA T 023618 (to G.H.), the USPHS AR 22031 and NSF MCB-9630997 grants (to E.R.), and USPHS grant AR 42023 (to E.H.E.).

‡ University of California.

§ University of Minnesota Medical School.

|| Eötvös Lorand University.

⊥ Permanent address: Department of Oral Biology, Hebrew University Hadassah School of Dental Medicine, Jerusalem 91120, Israel.

[1] Abbreviations: ANP, 4-azido-2-nitrophenyl-putrescine; 5-IAF, 5-iodoacetamido-fluorescein; pPDM, N,N′-*p*-phenylenebismaleimide; TG-ase, Ca^{2+}-independent bacterial transglutaminase; F-actin, filamentous (polymerized) actin; G-actin, monomeric actin; ANP-actin, ANP-labeled actin; HMM, heavy meromyosin; S1, myosin subfragment-1.

10.1021/bi981286b CCC: $15.00
Published on Web 12/03/1998

Direct and indirect evidence on myosin-induced changes in subdomain 2 and the C-terminus of actin (*19*−*24*) is also adding interest in the dynamic changes in F-actin. Orlova and Egelman (*7*) speculated that myosin binding may induce a rotation of subdomain 2 in F-actin. The rigor binding of myosin to F-actin may be cooperative under some conditions (*5*, *25*, *26*) and/or can induce cooperative changes in F-actin. The possible coupling between actin dynamics and function has been tested via modifications of actin. These studies established that proteolytic (*27*) and cross-linking modifications of F-actin (*28*, *29*) can be made that inhibit actomyosin motility without much change in the binding of myosin to actin and the actomyosin ATPase.

The cross-linking approach is particularly well-suited for probing the relationship between actin function and its structural dynamics. Selected sites on actin monomers can be chemically linked to abolish or inhibit structural rearrangements in the filaments. However, among the reagents used so far, only *p*-phenylenedimaleimide has the desirable specificity and cross-links adjacent actins on the two strands of F-actin, between C374 and K191 (*30*). This reaction appears to have little effect on actin's motility (*28*). Other actin cross-linkings, by glutaraldehyde and carbodiimide, inhibit the actomyosin motility, but the low specificity and unassigned sites of these reactions on actin complicate their interpretation.

In this study we took advantage of the specific intrastrand cross-linking between Q41 and C374 on adjacent actins by ANP (*4*) to connect between and restrict the mobility of the two dynamic regions on actin discussed above, the C-terminus and the DNase I loop on subdomain 2. The results of functional studies on the cross-linked actin are reported in this work.

MATERIALS AND METHODS

Reagents. Distilled and Millipore-filtered water and analytical grade reagents were used in all experiments. ATP, DTT, β-mercaptoethanol, phalloidin, and *N*,*N*′-*p*-phenylenebismaleimide were purchased from Sigma Chemical Co. (St. Louis, MO). 5-Iodoacetamidofluorescein and rhodamine phalloidin were obtained from Molecular Probes (Eugene, OR). 4-Azido-2-nitrophenyl-putrescine was synthesized as described by Hegyi et al. (*4*). Ca^{2+}-independent bacterial transglutaminase was a generous gift of Dr. K Seguro, Ajimoto, Co., Inc. (Kawasaki, Japan).

Proteins. Rabbit actin and myosin were prepared from rabbit skeletal muscle according to the methods of Spudich and Watt (*31*) and Godfrey and Harrington (*32*), respectively. S1 and HMM from rabbit myosin were prepared following the procedures of Weeds and Pope (*33*) and Margossian and Lowey (*34*), respectively.

ANP Labeling of Actin and UV Cross-Linking of ANP F-actin. G-actin (2 mg/mL) in G-buffer (4.0 mM Tris-HCl, pH 7.6, 0.4 mM ATP, and 0.2 mM $CaCl_2$) was incubated in the presence of ANP (8 M excess) and TG-ase (0.3 units/mL) at 4 °C overnight. This labeling procedure yields between 0.7 and 0.95 mol of ANP incorporated into G-actin, as measured by visible absorption of the label at 470 nm. To obtain various degrees of actin cross-linking, we copolymerized ANP G-actin by 2.0 mM $MgCl_2$ with different amounts of unlabeled G-actin. The resulting F-actin was pelleted by centrifugation at 40 000 rpm for 2 h in a Beckman 55.2 Ti rotor. The orange−red F-actin pellet was homogenized in F-buffer (4.0 mM Tris-HCl, pH 7.6, 0.2 mM ATP, and 2.0 mM $MgCl_2$) and then incubated for 1−2 h on ice in the dark. The photo-cross-linking of ANP-F-actin solution was carried out as described in the preceding paper (*4*). Aliquots of the reaction were denatured and examined on SDS−PAGE to determine the percentage of actin cross-linking. That percentage was defined as being equal to the percentage decrease in the intensity of the actin monomer band in the cross-linked sample relative to that in the un-cross-linked actin.

Thermostability of Actin. The thermostabilities of ANP cross-linked (90%) and un-cross-linked F-actin were compared in acto-S1 ATPase assays after heat treatment of actin at 60 °C (21) and in CD melting experiments. The unfolding of actin is accompanied by the loss of its ability to activate S1 ATPase activity (*21*). Thus, actin solutions (16 μM) were heated at 60 °C and aliquots were removed at different times for measurements of acto-S1 ATPase activity at 25 °C. The melting points of the cross-linked and un-cross-linked F-actin were determined by monitoring the changes in protein ellipticity at 222 nm in a Jasco J-600 spectropolarimeter (Japan Spectroscopic Co., Ltd.). The F-actin samples (4.0 μM) were heated in a 1 mm pathway cuvette at a constant rate of 1 °C/min up to 80 °C. The melting temperature was determined from derivative plots of ellipticity changes as a function of temperature. EPPS (5.0 mM), pH 7.5, containing 0.2 mM ATP, 0.2 mM β-mercaptoethanol, and 2.0 mM $MgCl_2$ was used as a buffer in all experiments involving heat treatment of actin.

Fluorescence and Light-Scattering Measurements. Both assays were carried out in a Spex Fluorolog spectrofluorometer (Spex Industries, Inc., Edison, NJ) at 25 °C in 250 μL cuvettes. The excitation wavelengths were set at 350 and 490 nm, and emissions were monitored at 350 and 515 nm for the light-scattering and the 5-IAF fluorescence assays, respectively.

S1 Binding Experiments. 5-IAF-labeled S1 was used for measuring S1 binding to actin. The labeling of S1 was required because the standard analysis of S1 bound to actin by SDS−PAGE is complicated by similar electrophoretic mobility of S1 and ANP cross-linked actin dimers. 5-IAF modification of SH1 groups on S1 was carried out as described by Schwyter at al. (*35*). Co-sedimentation assays for the binding of 5-IAF-labeled S1 to 4.0 μM phalloidin-stabilized F-actin were carried out at 23 °C in 4.0 mM Tris-HCl, pH 7.6, 2.0 mM $MgCl_2$, and 100 mM KCl. 5-IAF S1 and F-actin mixtures were centrifuged in a Beckman Airfuge at 140000*g* for 15 min. The amounts of 5-IAF S1 bound to F-actin were determined by measuring the 5-IAF fluorescence of the resuspended pellets.

ATPase Assays. Actin-activated ATPase activity of S1 was determined under steady-state conditions at 25 °C by a colorimetric assay in solutions containing 0.3 μM S1, 3.0 mM ATP, 3.0 mM $MgCl_2$, 10 mM KCl, 10 mM imidazol, pH 7.0, and varius concentrations of cross-linked and un-cross-linked F-actin. The ATPase data were fitted to the Michaelis−Menten equation to obtain values for K_m and V_{max} by using Sigma Plot II for Windows.

Acto-S1 ATPase was measured also for S1 complexes with filaments reassembled from the purified cross-linked actin

dimers, trimers, and oligomers. The purification of these materials is described in the companion paper (*36*). Because of limited quantities of such actin, the acto-S1 ATPases were obtained in these cases by monitoring the clearing time of 1.0 μM solutions of F-acto-S1 after the addition of 0.4 mM ATP. Control light-scattering measurements with solutions of un-cross-linked 1.0 μM F-acto-S1 showed a linear dependence of the clearing time on ATP concentrations between 0.2 and 1.0 mM. Clearing time is defined as the time during which the light scattering of acto-S1 is decreased by ATP to that of the sum of individual F-actin and S-1 light-scattering contributions. Upon hydrolysis of ATP the light scattering of the acto-S1 solution increases sharply leading to a determination of the clearing time, that is, the time of ATP hydrolysis.

In Vitro Motility Assays. In vitro motility assays were performed at 25 °C as described previously (*37*). Unless indicated otherwise, HMM at a concentration of 300 μg/mL was adsorbed to the nitrocellulose-coated coverslips. In all experiments ATP-desensitized HMM was removed from stock solutions by pelleting HMM in the presence of actin and ATP (*38*, *39*). All procedures, including the use of rhodamine phalloidin and the composition of the solutions, were the same as those described previously (*37*). The composition of the 50 mM ionic strength assay solution was 25 mM MOPS, pH 7.4, 25 mM KCl, 2.0 mM $MgCl_2$, 2.0 mM EGTA, 1.0 mM ATP, and the glucose−oxidase−catalase system to slow photobleaching. Methylcellulose (0.4%) was present in all solutions. Quantification of the sliding velocities of actin filaments was done with an Expertvision system (Motion Analysis, Santa Rosa, CA). Uniformly moving filaments are defined in this work as those with an SD of less than 0.3× the mean speed (*39*). pPDM-HMM was prepared as described by Chalovich (*40*) with modifications (*41*). pPDM-HMM was mixed at different concentrations with 200 μg/mL of HMM prior to their adsorption to coverslips to generate external load in the motility assays.

Electron Microscopy. The ANP cross-linked Mg^{2+}-actin filaments used for electron microscopy were prepared as described above, while control un-cross-linked Mg^{2+}-actin filaments were prepared from the same actin preparations as the cross-linked filaments, using the procedure described in Orlova and Egelman (*7*). Samples were diluted to a final concentration of 0.05−0.1 mg/mL with polymerization buffers and applied to lightly glow-discharged carbon-coated grids. The samples were then washed with 3−5 drops of the polymerization buffer and negatively stained with 2% (w/v) uranyl acetate. A JEOL 1200EXII electron microscope was used at an accelerating voltage of 80 kV, at a magnification of 30000×, and with a typical defocus of less than 0.5 μm. Minimal dose procedures were employed, such that specimens received no irradiation at high magnification prior to the recording of images on film. Electron micrographs were scanned with an Eikonix 78/99 digital camera, resulting in a sampling of about 3.0 Å/pixel. The exact magnification was determined from the 23 Å pitch helix of tobacco mosaic virus (TMV) particles co-prepared with the actin.

Filament images were straightened (*42*), and images were processed as described in Orlova and Egelman (*6*). Three-dimensional surfaces were generated with a Marching Cubes algorithm (*43*) and rendered with the Advanced Visualizer software (Wave front Technologies).

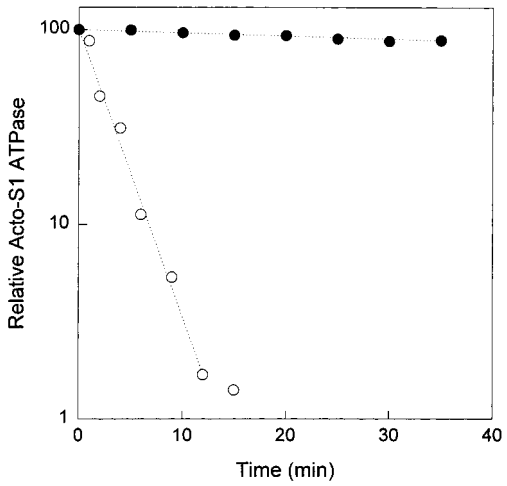

FIGURE 1: Semilogarithmic plot of the S1 ATPase activation by actin as a function of the incubation time of F-actin at 60 °C: ○, F-actin; and ●, extensively (90%) cross-linked ANP-F-actin. Actin concentration during the heat treatment was 18 μM, and the concentrations of S1 and actin in the ATPase assays (at 25 °C) were 0.3 and 9.0 μM, respectively. The first-order rates of the loss of ATPase activation obtained from the slopes of the straight lines were 0.340 and 0.003 min^{-1} for F-actin and cross-linked ANP-F-actin, respectively. (A 90% cross-linked ANP-F-actin contains according to SDS−PAGE 10% of total actin in the form of un-cross-linked monomers).

RESULTS

Structural Properties of ANP Cross-Linked F-actin. Several previous studies provided evidence for the high sensitivity of actin filament stability and structure to modifications or cleavage at the C-terminus (*8*, *44*, *45*) and the DNase I loop in subdomain 2 of actin (*7*, *15*, *46*, *21*). These results and the likely involvement of the C-terminus and the DNase I loop in intermolecular interactions in F-actin suggested that the cross-linking of these regions may change filament stability.

Figure 1 shows the effect of ANP cross-linking on the functional thermostability of F-actin. Clearly, the un-cross-linked F-actin loses its ability to activate S1 ATPase activity much faster than the cross-linked actin when both are heated at 60 °C. The rates of thermal "inactivation" of the cross-linked and un-cross-linked F-actin at 60 °C (0.003 and 0.34 min^{-1}, respectively) differ by a factor of about 100 (Figure 1). Consistent with this observation, CD melting experiments show a shift of 11 °C in the melting point of F-actin, from 63 to 74 °C, upon its cross-linking by ANP (Table 1). The cross-linking also sharpened notably the melting transition of F-actin indicating increased cooperativity of actin unfolding (data not shown). It appears that the cross-linking increases the structural uniformity of F-actin which can normally equilibrate among multiple conformational states of subdomain 2 (*7*).

Electron Microscopy and Three-Dimensional Reconstruction. In an effort to see if the cross-linking introduces significant structural perturbations into F-actin, we have used electron microscopy and three-dimensional reconstruction techniques to visualize the filaments. Filament images were Fourier transformed, and the axial spacings of the layer lines

Table 1: Effect of ANP Cross-Linking on the Properties of F-actin[a]

		rigor IAF-S1 binding	Acto-S1 ATPase	
F-actin	T_m (°C)	K_d (μM)	V_{max} (s^{-1})	K_m (μM)
un-cross-linked	63 ± 2	1.0 ± 0.1	13.0 ± 0.6	18.3 ± 2.1
cross-linked (50%)		1.1 ± 0.1	10.3 ± 0.7	20 ± 3.0
cross-linked (90%)	74 ± 3	1.0 ± 0.1	6.5 ± 0.8	25 ± 3.6

[a] T_m values, the melting temperatures of F-actin, were obtained from CD experiments by determining the temperatures of ellipticity transitions at 222 nm for un-cross-linked and a 90% cross-linked F-actin. K_d values for rigor binding of IAF-S1 to actin and the V_{max} and K_m values for acto-S1 ATPases were determined for F-actin and 50% and 90% ANP cross-linked F-actin.

contained within these transforms were used to estimate the twist of the actin filaments in subunits per turn of the 5.9 nm pitch left-handed helix. The control filaments ($n = 125$) had 2.1677 ± .0061 (SD) subunits/turn, while the cross-linked filaments ($n = 147$) had 2.1626 ± .0062 (SD) subunits/turn. This shift is highly significant statistically ($p \ll 0.001$) and corresponds to a change in average angular rotation between adjacent subunits (separated by a 2.7 nm axial rise) of about 0.4°, or a rotation of about 0.8° between neighboring subunits along the same long-pitch helical strand.

Individual filaments were selected for further processing on the basis of the number of visible and symmetrical layer lines. Following procedures previously described (*6*−*8*, *47*), we generated an average of 19 filaments for the un-cross-linked control and 26 cross-linked filaments. Eight layer lines were extracted for each filament ($L = 0$, $n = 0$; $L = 1$, $n = 2$; $L = 2$, $n = 4$; $L = 5$, $n = -3$; $L = 6$, $n = -1$; $L = 7$, $n = 1$; $L = 8$, $n = 3$; $L = 13$, $n = 0$). The averaging statistics for these layer lines were very similar for the two different populations, with an *F*-weighted up−down phase residual (*47*) of 49° versus 75° for the control, and 50° versus 76° for the cross-linked filaments. This statistic reflects the strength of the intrinsic structural polarity, the signal-to-noise ratio, and the homogeneity of the samples, and the fact that it is so similar for both populations suggests that these three parameters have not been greatly changed.

Figure 2 shows the rendered surfaces from the three-dimensional reconstructions of the control and cross-linked filaments, (88% cross-linked) while Figure 3 shows cross-sectional contour plots from the same reconstructions. The contour plots show that the resolution of the reconstructions is sufficient to resolve the subdomains of the actin protomer. The reconstructions show that there are no gross changes in F-actin structure, but they also reveal two differences that were deemed to be significant. The first (arrow A, Figure 2) involves a decrease of connectivity between the two long-pitch helical strands, while the second (arrow B, Figure 2) involves a change in the orientation of subdomain 2.

Could the differences observed between the two populations be due to differences in resolution? A comparison of the *R*-weighted power contained in the averaged layer lines (data not shown) suggests that this is not the case, since both reconstructions appear to be of comparable resolution.

Solution Interactions with S1. The rigor (in the absence of nucleotides) and weak (in the presence of MgATP) binding of 5-IAF-labeled S1 to F-actin was determined by cosedimentation assays. The same actin preparations but

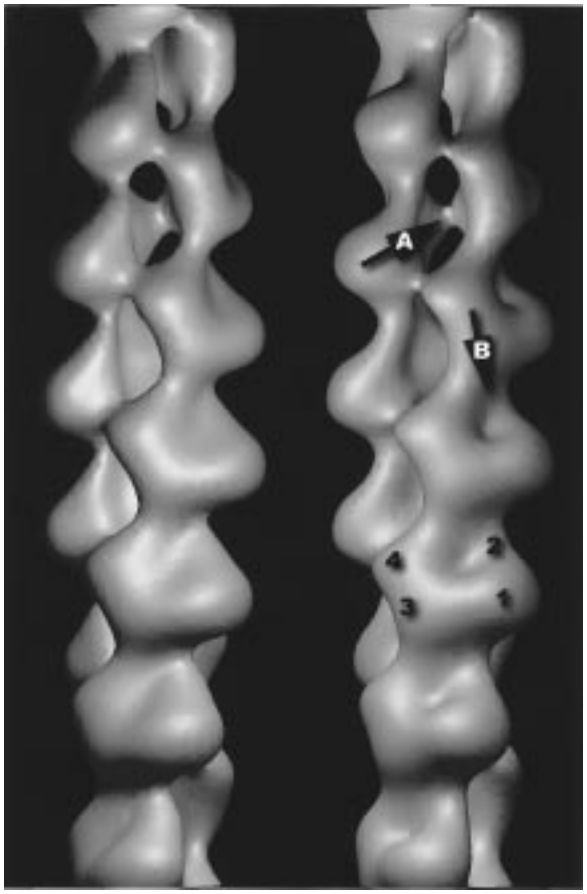

FIGURE 2: A comparison of the rendered surfaces for control filaments (left) and extensively (88%) cross-linked filaments (right). The two arrows indicate the main difference seen between these two populations: (A) a reduction in the connectivity between the two long-pitch helical strands; and (B) a change in the conformation of subdomain-2 and the nucleotide-binding cleft. Numbers 1 through 4 indicate the subdomains of actin. The surfaces were generated by choosing a threshold that yielded about 115% of the expected molecular volume, using a partial specific volume for protein of 0.75 cm^3/g.

unlabeled S1 were used in the measurements of acto-S1 ATPase activity. Surprisingly, none of the tested parameters was significantly affected by a 50% (±5%) cross-linking of actin (Table 1), that is, for actin filaments containing ~ 50% un-cross-linked monomers (according to SDS−PAGE analysis). The small change in the V_{max} value is similar to the changes observed for actin labeled at Cys-374 with some fluorescent compounds (*12*). The K_m values (Table 1) and the results of cosedimentation of acto-S1 in the presence of MgATP (now shown) indicate virtually no change in the weak binding of S1 to F-actin after its cross-linking. Similarly, the cross-linking does not alter the rigor binding of S1 to actin (Table 1) (which is reduced by 5-IAF labeling of S1; ref *35*). However, these results do not exclude the possibility that the intrastrand cross-linking of the DNase I binding loop and the C-terminus of adjacent actins might change individual rate constants of the cross-linked monomers for acto-S1 binding and dissociation without obvious effects on the equilibrium constants.

More extensive cross-linking of actin, up to 90% (+5%), did not result in any significant changes in rigor S1 binding but caused about 50% decrease in the V_{max} value of acto-S1 ATPase (Table 1).

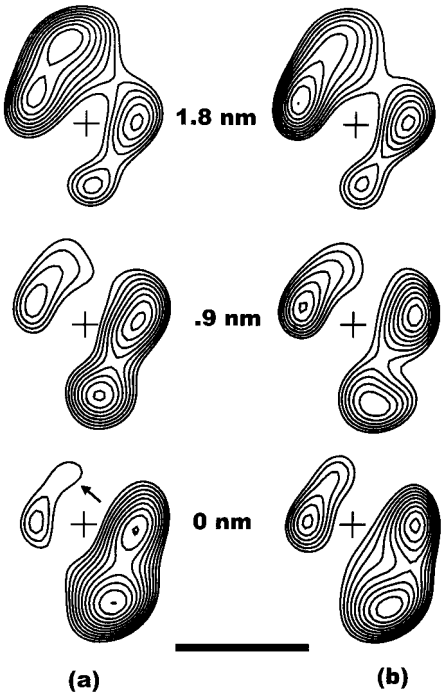

FIGURE 3: The cross-sectional contour plots of the reconstruction in Figure 2: (a) control filaments; (b) cross-linked filaments. The sections have been cut at a spacing of 0.9 nm. Given the helical symmetry of actin, the next section at 2.7 nm would be the same as the section at 0 nm, but rotated by about 167°. The helical axis is indicated by the cross in each section, and the scale bar is 50 Å. The arrow in (a) indicates the density due to subdomain 2 in the control filament, and it can be seen that this density is significantly weaker than the corresponding region in the cross-linked filament (b). The increase in density in this region in the cross-linked filament could be due to either a change in the orientation of subdomain 2 or a stabilization of this subdomain.

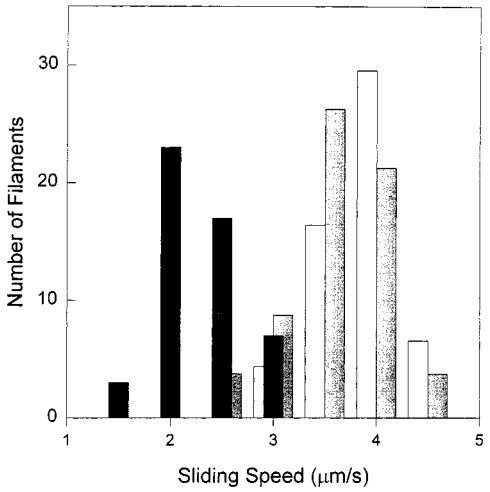

FIGURE 4: Effect of ANP cross-linking on the in vitro motility properties of F-actin. The plot shows distributions of speeds for uniformly sliding F-actin (white bars), 95% labeled and un-cross-linked ANP-F-actin (gray bars), and 50% cross-linked ANP-F-actin (black bars). Mean sliding speeds for F-actin, ANP F-actin, and cross-linked ANP F-actin are 4.2 ± 0.8, 4.1 ± 0.8, and 2.7 ± 0.6 μm/s, respectively.

In Vitro Motility of ANP-F-Actin. The effect of ANP cross-linking (50%) on the sliding speed of F-actin is shown in Figure 4. The mean sliding speeds of the un-cross-linked and cross-linked filaments were 4.2 ± 0.8 and 2.7 ± 0.6 μm/s, respectively. This decrease in the speed was accompanied by a parallel decrease (35%) in the number of sliding filaments. ANP labeling (95−100%) of Gln-41, without the subsequent cross-linking, caused only a minor, if any, decrease in the motility of F-actin to a mean sliding speed of 4.1 ± 0.8 μm/s. These results show that ANP cross-linking of F-actin and not the labeling of Gln 41 inhibits the sliding of actin filaments in the in vitro motility assays. Furthermore, they show that ANP cross-linking of F-actin (50%) impacts its motile properties without obvious changes in the activation of S1 ATPase and S1 binding by actin (Table 1). As shown in Figure 5, the 90% cross-linked F-actin (10% un-cross-linked monomers) is virtually immobile; very few filaments slide (<5%), and those that do move at very low speeds. Thus, complete movement inhibition of F-actin can be achieved via its cross-linking by ANP.

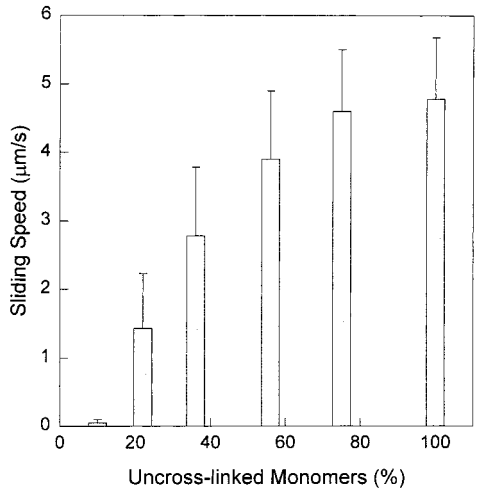

FIGURE 5: Dependence of the motility of F-actin on the extent of its cross-linking by ANP. Mean speeds of uniformly sliding filaments were determined as a function of the un-cross-linked monomer present in these preparations (The percentage of un-cross-linked monomers was determined by SDS−PAGE).

Some possible reasons for the inhibition of actin sliding by ANP cross-linking were tested in the in vitro motility assays by changing the standard conditions of these experiments. The deletion of methyl cellulose from the assays had no effect on the sliding of cross-linked and un-cross-linked filaments (at 50 mM ionic strength). This supports the solution results (K_m and cosedimentation) that the ANP cross-linking does not impair significantly the weak acto-S1 binding. When the weak binding is decreased, for example by tryptic cleavage of loop 2 (the 50:20 kDa junction) in HMM (*57*) or charge substitutions in yeast actin (*37*, *48*), the absence of methyl cellulose in the assay leads to motility loss due to diffusion of actin filaments.

The possibility that the cross-linked actins in F-actin bind HMM especially strongly and thus introduce load into the assay, which slows the motion generated with HMM by the un-cross-linked segments of filaments, is addressed by monitoring the sliding speeds of F-actin versus the percentage of its cross-linking. Figure 5 shows the results of such experiments and reveals only a small inhibition of actin motion at up to 25% cross-linking of F-actin (75% un-cross-linked monomers). The observed dependence of actin speeds on the percentage of actin cross-linking (Figure 5) virtually rules out a mechanism by which motion is arrested due to a "trap" of rigor complexes of HMM with the cross-linked

actins. As shown by Cuda et al. (*49*) rigor bond type inhibition of actin motion would yield a much stronger decrease in the sliding of filaments with an increase in the percentage of cross-linking than that shown in Figure 5. The decrease in the percentage of moving filaments in these assays with a decrease in the percentage of un-cross-linked actin was similar to that shown for filament speeds in Figure 5.

A variation on the scenario of a rigor trap for HMM is that only a small fraction of cross-linked actin does not detach well from HMM and, thus, arresting the movement of actin requires its greater cross-linking. To test for this possibility, HMM at different concentrations was added also to the motility assay solutions. The rationale behind this experiment was that the added HMM would block the "trapping" monomers on F-actin and consequently accelerate the movement of the cross-linked filaments. However, the only effect of the added HMM was to slow the sliding of the cross-linked and un-cross-linked filaments by a similar factor (data not shown). This slowing of sliding is probably due to the competition for actin between the HMM in solution and the motion-generating HMM on the coverslip surface and indicates the absence of rigor-like traps for HMM on the cross-linked actin.

Force Measurements. At sufficient density of HMM on the coverslip surface actin filaments slide at a speed $V_f = d/t_s$, where d is the mean step size per cross-bridge and t_s is the duration of the power stroke (*50*). Clearly, one mechanism by which the speed of actin filaments may be reduced is via an increase in the fraction of time (out of the total cycle time) in which cross-bridges generate motion. Such an increase in t_s can be related to a decrease in the rate of cross-bridge detachment from actin or ADP release from actomyosin. The consequent increase in the population of cross-bridges in the force-generating steps should lead to an increased force production at the same time as the unloaded sliding velocity of the actomyosin system is decreased.

To test whether the slow sliding of cross-linked actin over HMM can be related to an increased duration of force-generating complexes, we measured the relative forces developed by HMM with the cross-linked and un-cross-linked actin by monitoring their motion against external load. As in previous studies, in which NEM-HMM was used to produce the load (*37, 41, 51, 52*), the amount of load-producing HMM needed to halt actin movement is a measure of the force exerted by the unmodified HMM. The external load was generated by adsorbing to the coverslip surface different amounts of pPDM-modified HMM which is catalytically inactive but binds actin weakly. As shown in Figure 6, both the sliding speed (A) and the percentage of filaments sliding (B) decrease linearly with an increase in the concentration of the pPDM-HMM solution used for the adsorption of modified HMM (in the presence of 200 μg/mL HMM) to the coverslip surface. Both plots yield similar extrapolated values; the movement of cross-linked and un-cross-linked actin stops at 250 $\pm$ 20 and 325 $\pm$ 35 μg/mL pPDM-HMM, respectively. This means that the 50% cross-linked actin generates with HMM only 75% of the force exerted with un-cross-linked actin. Simple changes in t_s cannot account for both the force and sliding speed decreases with the cross-linked actin.

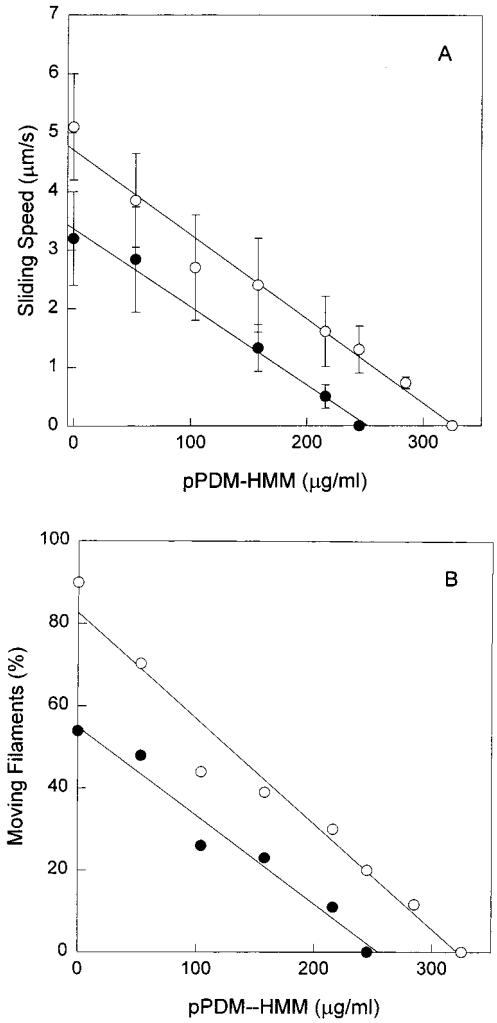

FIGURE 6: Effect of ANP cross-linking of F-actin on the relative force produced with HMM as measured by the pPDM-HMM load. (A) Mean sliding speeds versus the concentration of pPDM-HMM applied to the assay surface. (B) Percentage of the filaments moving versus the concentration of pPDM-HMM applied to the assay surface: ○, F-actin; ●, 50% cross-linked ANP-F-actin. The concentration of HMM applied to the assay surface was 200 μg/mL. The sliding of between 100 and 300 filaments was monitored in each case.

The force and speed changes observed for the cross-linked actin raise the possibility of an effective decrease in the number of force-generating cross-bridges. This possibility was tested further by comparing the dependence of cross-linked and un-cross-linked actin sliding speeds on the HMM concentration. As expected, a decrease in HMM concentration from 300 to 50 μg/mL had only a small effect on the speed of un-cross-linked actin (Figure 7). The sliding speed of the cross-linked actin showed a considerably steeper dependence on HMM concentration. This type of behavior would be observed with un-cross-linked actin only in the lower range of HMM concentrations (0$-$100 μg/mL). Thus, it appears that at least some aspects of the mechanical performance of HMM with cross-linked actin can be modeled by lowering the effective HMM concentration on the coverslip surface.

In vitro Motility of Actin Filaments Assembled from Cross-Linked Actin Dimers, Trimers, and Oligomers. The ANP cross-linked filaments used up to now contain random sequences of un-cross-linked monomers and cross-linked

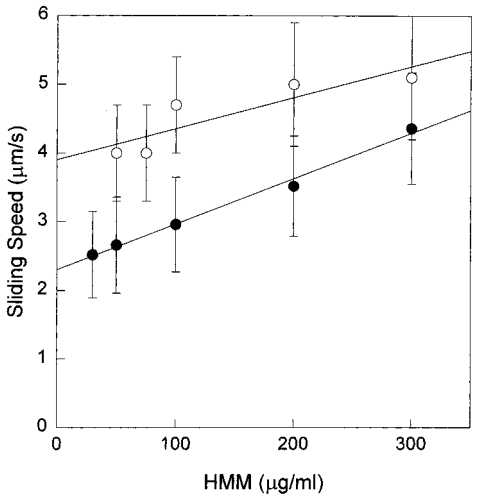

FIGURE 7: Effect of ANP cross-linking of F-actin on the sliding speed of actin in the in vitro motility assays at different HMM concentrations. HMM concentrations are those of the solutions used for the adsorption of HMM to the assay surface: ○, F-actin; ●, 50% cross-linked ANP-F-actin.

dimers, trimers, and higher oligomers. Differences in the distribution of actin monomers among the different cross-linked species may introduce obvious variations in filament properties. Both the number and the distribution of un-cross-linked actin−actin contacts in the filament and the length of the blocks of such un-cross-linked contacts may determine the motile properties of these filaments. To examine the inhibition of actin filament movement via well-controlled changes in the frequency of un-cross-linked actin−actin contacts (within the same strand), we formed actin filaments from the purified cross-linked dimers, trimers (with ∼10% contamination by dimers and oligomers), and oligomers. In the filaments made of cross-linked dimers every other actin−actin intrastrand interface is un-cross-linked while in filaments of trimers every third such contact is un-cross-linked. In electron micrographs these filaments do not appear different from un-cross-linked actin filaments except for their greater tendency to bend and for the presence of shorter filaments (*36*).

Because of a limited supply of cross-linked actin multimers only those experiments which do not require much actin were carried out with the reassembled filaments. The acto-S1 ATPases of filaments made of dimers, trimers, and oligomers were approximately the same for all of them, as determined by the clearing time of these solutions (∼0.5 s^{-1}). This activity was about 2-fold lower than that obtained with un-cross-linked actin (Table 2), perhaps because of the additional manipulations and the time involved in the purification of these species (*36*). The rigor binding of S1 to F-actins, monitored by light-scattering measurements, was similar for all actins (data not shown). However, in vitro motility assays revealed large differences between these F-actins. The dimer-made filaments moved over the HMM surface at about 40% lower mean speeds that those of un-cross-linked filaments (Table 2). The mean speed of all moving cross-linked trimer-made filaments is reduced even more, between 70% and 75%, when compared to the speed of un-cross-linked actin. Furthermore, close to 50% of trimer-made filaments do not move in the motility assays and none of the filaments made from cross-linked oligomers moves in these experiments (Table 2). When uniformly moving filaments are selected for analysis, only 12% of trimer-made filaments satisfy the criteria of such movement while about 70% of dimer-made filaments still move uniformly (Table 2). These results show a progressive loss of actin's motility with the increase in the length of the cross-linked actin oligomers despite the invariant acto-S1 ATPase and rigor S1 binding of F-actin reassembled from such cross-linked actins.

DISCUSSION

Electron microscopy and three-dimensional reconstructions of ANP cross-linked F-actin eliminate the possibility that this cross-linking introduces a large structural change in F-actin. The change seen in the conformation of subdomain 2 is not unexpected; this subdomain is the most labile part of the F-actin structure (reviewed in ref *53*), and it contains one site of the cross-linking (Gln-41). The change observed in the interstrand connectivity, although somewhat unexpected, is consistent with the previously observed destabilization of actin filaments by the removal of two or three C-terminal residues in actin (*42*, *45*, *54*). It has been shown that this destabilization appears to occur by a weakening of the interstrand connectivity (*47*). Since these C-terminal residues are not located near the filament axis (*16*), and since the shift in mass seen at low resolution involves much more than two or three residues, the cleavage of these residues appears to generate an allosteric conformational change in the actin filament (*47*). The cross-linking between the C-terminus (Cys-374) and subdomain 2 on another subunit appears to introduce a similar conformational change in the filament.

The main result of this part of the work is that intrastrand cross-linking of adjacent actin monomers in F-actin, but not the labeling of Gln-41 alone, inhibits motion and force generation by the actomyosin system. This effect is documented most extensively on preparations of ∼50% cross-linked actin, that is, actin filaments which contain ∼50% un-cross-linked monomers and, thus, a greater percentage of un-cross-linked subdomain 2/C-terminus interfaces. The rationale for the choice of ∼50% cross-linked actin is that such filaments still exhibit sufficiently uniform and fast motion in the motility assays for accurate measurements of motion inhibition by the external load generated by pPDM-HMM. The measurements in the presence of pPDH-HMM provide an estimate of relative forces developed by acto-myosin and are similar to relative force measurements made by using NEM-HMM load in motility assays (*37*, *41*, *51*, *52*).

As argued in the Results, the simultaneous decrease (by ∼25%) in the relative force produced by HMM and the ∼50% cross-linked F-actin and in the sliding speed of these filaments in the absence of load (by ∼ 35%) cannot be accounted for by postulating a change in t_s alone, the duration of the force-generating steps in the cross-bridge cycle. In principle, a reduction in force may result from a decrease in either one or both of the unitary force generated per power stroke and the flux of HMM cross-bridges through the cycle. The loss of motility for ≥90% cross-linked filaments suggests that actomyosin interactions are mechanically unproductive for such a system; that is, the unitary force produced by HMM and the cross-linked stretch of actin is

Table 2: Actin Filaments Assembled from Cross-Linked, Purified Dimers, Trimers, and Oligomers: Acto-S1 ATPase and Actin Sliding in the in Vitro Motility Assays[a]

F-actin composition	ATPase (s^{-1})	filaments moving (%)		mean speed (μm/s)	
		all moving filaments	moving uniformly	all moving filaments	moving uniformly
un-cross-linked actin	1.01	100	88	3.8 ± 1.0	4.0 ± 0.9
cross-linked dimers	0.52	100	70	2.3 ± 0.4	2.4 ± 0.4
cross-linked trimers	0.48	52	12	1.0 ± 0.8	2.2 ± 0.4
cross-linked oligomers	0.48	0	0	0.0	0.0

[a] The rates of acto-S1 ATP hydrolysis were determined as described in Materials and Methods by light-scattering determination of the clearing time of equimolar (1.0 μM) mixtures of S1 and F-actin after the addition of 0.4 mM ATP. Filaments of cross-linked actin were obtained by the polymerization of purified cross-linked dimers, trimers, and oligomers with 2.0 mM $MgCl_2$. ATPase activities are expressed as turnover rates (micromoles of P_i per micromole S1 per second). In vitro motility of actin filaments was monitored as described in Materials and Methods. Uniformly moving filaments are those filaments for which the ratio of the SD of their speed/mean speed is smaller or equal to 0.3 (*39*).

either small or 0. The ~50% cross-linked filament contains probably some fraction of such mechanically inactive actin, thereby decreasing the effective or productive flux of HMM cross-bridges through the cycle. Because single molecule measurements are not easily accessible at present, helpful insight into this issue can be sought in motility assays carried out at various densities of HMM on the motility surface. Thus, if the ~50% cross-linking of F-actin would decrease by 25% (Figure 6) only the unitary force developed per acto-HMM interaction with such filaments, one might expect that their sliding speed over HMM, albeit lower than that of un-cross-linked F-actin, would be equally insensitive to HMM density on the motility surface. In fact, the higher dependence on HMM concentration of the movement of cross-linked than un-cross-linked F-actin implies a decreased flux of force-producing HMM through the cross-bridge cycle with the cross-linked actin. The decrease in flux may result from changes in the rate constant(s) of some steps in the cycle or from the mechanically unproductive interaction of HMM with the cross-linked segments of actin. In the later case, if the cross-linked actin units execute a mechanically futile cycle, motion and force would be generated only by un-cross-linked actin monomers.

If the decrease in the relative force (~25% for the 50% cross-linked filaments) describes the percentage loss of force-generating acto-HMM interactions, why does the speed of these cross-linked filaments decrease by so much (up to 35% for the 50% cross-linked actin)? A simple answer might be that the cross-linking evokes a combination of responses in actin. In addition to mechanical inactivation of a fraction of actin in the filaments, another fraction could show increased t_s, leading to a greater net decrease in the filament speed than in the force produced with HMM. Quantitative analysis of the force and speed parameters could be complicated also if a weak load is produced by the mechanically inactivated actin.

The experiments with filaments assembled from cross-linked dimers, trimers, and oligomers illuminate another aspect of motion and force inhibition via ANP cross-linking of actin. All of these filaments do not contain un-cross-linked actin monomers, that is, according to the terminology used up to now, they are 100% cross-linked. Yet, while dimer-made filaments move still well (at ~50% sliding speed of un-cross-linked actin), the trimer-made filaments barely move, and the oligomer-made filaments do not move at all. At the same time, the limited tests that could be done with the small amounts of such filaments (preparative constraints involved in the purification of the cross-linked species are elaborated in the companion publication; ref *36*) do not reveal any differences in S1 binding (rigor) and acto-S1 ATPase among them. Clearly, the dimer-, trimer-, and oligomer-made filaments differ from each other in the percentage of un-cross-linked subdomain 2/C-terminus interfaces (50%, 33%, and <33%, respectively). The sliding of actin over HMM decreases sharply when the percentage of un-cross-linked interface decreases to ~33% and below.

The above considerations about inhibition of actin sliding and force production by ANP cross-linking of actin include: (i) the lack of strong effects on acto-S1 ATPase; (ii) little, if any, effect on strong and weak binding of S1; (iii) possible changes in the unitary forces and/or fluxes of HMM through the cycle; and (iv) the effect of length of the cross-linked blocks of monomers on the inhibition of actin sliding lead to the proposal of the uncoupling of mechanical and catalytic events in the cross-bridge cycle of cross-linked filaments. It is suggested that such uncoupling occurs due to the immobilization of the subdomain 2/C-terminus interface in F-actin. The dynamic properties of subdomain 2 are largely responsible for transitions between conformational states of F-actin (*52*) and are the main basis for two different conformations of G-actin observed by X-ray crystallography (*55*, *56*). It has been speculated that such transitions are important for motion and force generation and that they may need to be "synchronized" with conformational transitions in S1 during the cross-bridge cycle. Our results suggest that, while the blocking of such actin transitions does not impair much acto-S1 interactions in solution, it uncouples the mechanical and catalytic events.

It is also apparent that the mechanical deactivation of F-actin increases with the length of the cross-linked block of actin monomers. This can be easily rationalized if dynamic transitions along the subdomain 2/C-terminus interface are needed to release the cumulative strain in the structure of F-actin produced by myosin. Alternatively, it is possible that the cross-linking traps actin filaments in a strained conformation and the impact of longer stretches of cross-linked actins is more difficult to dissipate. In both cases such longer stretches of cross-linked actin could inhibit force generation by HMM with actins which are not cross-linked to each other. It is noted also that tampering with subdomain 2 integrity via subtilisin cleavage of DNase I loop leads to a strong inhibition of actin sliding (*27*). Thus, for different reasons, the cleaved actin, like the ANP cross-linked actin, may impair the structural adaptation of actin filaments to the changes in myosin needs for force generation during the cross-bridge cycle. However, on the side of caution, it should

be noted that electron microscopy shows some structural perturbation of F-actin caused by the cross-linking and leaves open the question of whether a conformational difference alone, such as the weakening of the interstrand connectivity, or the inhibition of dynamic changes in actin is responsible for the loss of force.

REFERENCES

1. Yount, R. G. (1993) *J. Muscle Res. Cell Motil. 14*, 547−551.
2. Cooke, R. (1995) *FASEB J. 9*, 636−642.
3. Oosawa, F. (1983) in *Muscle and non-muscle motility* (Stracher, A., Ed.) Vol. 1, pp 151−216, Academic Press, New York.
4. Hegyi, G., Mák, M., Kim, E., Elzinga, M., Muhlrad, A., and Reisler, E. (1998) *Biochemistry 37*, 17784−17792.
5. Oosawa, F., Fujime, S., Ishiwata, S., and Mihashi, K. (1972) *Cold Spring Harbor Symp. Quant. Biol. 37*, 277−285.
6. Orlova, A., and Egelman, E. H. (1992) *J. Mol. Biol. 227*, 1043−1053.
7. Orlova, A., and Egelman, E. H. (1993) *J. Mol. Biol. 232*, 334−341.
8. Orlova, A., and Egelman, E. H. (1995) *J. Mol. Biol. 245*, 598−607.
9. Muhlrad, A., Cheung, P., Phan, B. C., Miller, C., and Reisler, E. (1994) *J. Biol. Chem. 269*, 11852−11858.
10. Strzelecka-Golaszewska, H., Wozniak, A., Hult, T., and Lingberg, U. (1996) *Biochem. J. 316*, 713−721.
11. Egelman, E. H. (1997) *Structure 5*, 1135−1137
12. Crosbie, R. H., Miller, C., Cheung, P., Goodnight, T., Muhlrad, A., and Reisler, E. (1994) *Biophys. J. 67*, 1957−1964.
13. Strzelecka-Golaszewska, H., Moraczewska, J., Khaitlina, S. Y., and Mossakowska, M. (1993) *Eur. J. Biochem. 211*, 731−742.
14. Kuznetsova, I., Antropova, O., Turoverov, K., and Khaitlina, S. (1996) *FEBS Lett. 383*, 105−108.
15. Kim, E., and Reisler, E. (1996) *Biophys. J. 71*, 1914−1919.
16. Lorenz, M., Poole, K. J. V., Popp, D., Rosenbaum, G., and Holmes, K. (1995) *J. Mol. Biol. 246*, 108−119.
17. Tirion, M. M., Benavraham, D., Lorenz, M., and Holmes, K. C. (1995) *Biophys. J. 68*, 5−12.
18. Owen, C., and de Rosier, D. (1993) *J. Cell Biol. 123*, 337−344.
19. Duong, A., and Reisler, E. (1994) in *Actin: Biophysics, Biochemistry, and Cell Biology* Estes, J. E., and Higgins, P. J., eds.) pp 59-70, Plenum Press, NY.
20. Kouyama, T., and Mihashi, K. (1981) *Eur. J. Biochem. 114*, 33−38.
21. Kim, E., Miller, C. J., Motoki, M., Seguro, K., Muhlrad, A., and Reisler, E. (1996) *Biophys. J. 70*, 1439−1446.
22. Crosbie, R. H., Chalovich, J. M., and Reisler, E. (1992) *Biochem. Biophys. Res. Commun. 184*, 239−245.
23. Fievez, S., and Carlier, M. F. (1993) *FEBS Lett. 316*, 186−190.
24. Kasprzak, A. A., Takashi, R., and Morales, M. F. (1988) *Biochemistry 27*, 4512−4522.
25. Miki, M., Wahl, P., and Auchet, J. C. (1982) *Biochemistry 21*, 3661−3665.
26. Orlova, A., and Egelman, E. H. (1997) *J. Mol. Biol. 265*, 469−474.
27. Schwyter, D. H., Kron, S. J., Toyoshima, Y. Y., Spudich, J. A., and Reisler, E. (1990) *J. Cell Biol. 111*, 465−470.
28. Prochniewicz, E., and Yanagida, T. (1990) *J. Mol. Biol. 216*, 761−772.
29. Prochniewicz, E., Katayama, E., Yanagida, T., and Thomas, D. D. (1993) *Biophys. J. 65*, 113−123.
30. Elzinga, M., and Phelan, J. (1984) *Proc. Natl. Acad. Sci. U.S.A. 81*, 6599−6602.
31. Spudich, J., and Watt, S. (1971) *J. Biol. Chem. 246*, 4866−4871.
32. Godfrey, J. E., and Harrington, W. F. (1970) *Biochemistry 9*, 886−893.
33. Weeds, A., and Pope, B. (1977) *J. Mol. Biol. 111*, 129−157.
34. Margossian, S. S., and Lowey, S. (1982) *Methods Enzymol. 85*, 55−72.
35. Schwyter, D., Phillips, M., and Reisler, E. (1989) *Biochemistry 28*, 5889−5895.
36. Kim, E., Phillips, M. L., Hegyi, G., Muhlrad, A., and Reisler, E. (1998) *Biochemistry 37*, 17793−17800.
37. Miller, C. J., Wong, W. W., Bobkova, E., Rubenstein, P. A., and Reisler, E. (1996) *Biochemistry 35*, 16557−16565.
38. Kron, S., and Spudich, J. (1986) *Proc. Natl. Acad. Sci. U.S.A. 83*, 6272−6276.
39. Homsher, E., Wang, F., and Sellers, J. R. (1992) *Am. J. Physiol. 262*, C714−C723.
40. Chalovich, J., Greene, L., and Eisenberg, E. (1983) *Proc. Natl. Acad. Sci. U.S.A. 80*, 4909−4913.
41. Warshaw, D. M., Derosiers, J., Work, S., and Trybus, K. (1990) *J. Cell Biol. 111*, 453−463.
42. Egelman, E. H. (1986) *Ultramicroscopy 19*, 367−373.
43. Lorensen, W. E., and Cline, H. E. (1987) *Comput. Graph. 21*, 163−169.
44. O'Donoghue, S. I., Miki, M., and dos Remedios, C. (1992) *Arch. Biochem. Biophys. 293*, 110−116.
45. Mossakawska, M., Moraczewska, J., Khaitlina, S., and Strzelecka-Golaszewska, H. (1993) *Biochem. J. 289*, 897−902.
46. Khaitlina, S. Y., Moraczewska, J., and Strzelecka-Golaszewska, H. (1993) *Eur. J. Biochem. 218*, 911−920.
47. Orlova, A., Prochniewicz, E., and Egelman, E. H. (1995) *J. Mol. Biol. 245*, 598−607.
48. Miller, C. J., and Reisler, E. (1995) *Biochemistry 34*, 2694−2700.
49. Cuda, G., Pate, E., Cooke, R., and Sellers, J. R. (1997) *Biophys. J. 72*, 1767−1779.
50. Uyeda, T. Q. P., Kron, S. J., and Spudich, J. A. (1990) *J. Mol. Biol. 214*, 699−710.
51. Miller, C. J., Doyle, T. C., Bobkova, E., Botstein, D., and Reisler, E. (1996) *Biochemistry 35*, 3670−3676.
52. Haeberle, J. R. (1994) *J. Biol. Chem. 269*, 12424−12431.
53. Egelman, E. H., and Orlova, A. (1995) *Curr. Opin. Struct. Biol. 5*, 172−180.
54. Drewes, G., and Faulstich, H. (1993) *J. Biochem. 212*, 247−253.
55. Chik, J. K., Lindberg, U., and Schutt, C. E. (1996) *J. Mol. Biol. 263*, 607−623.
56. Schutt, C. E., Myslik, J. C., Rozycki, M. D., Goonesekere, N. C. W., and Lindberg, U. (1993) *Nature 365*, 810−816.
57. Bobkov, A. A., Bobkova, E. A., Lin, S. H., and Reisler, E. (1996) *Proc. Natl. Acad. Sci. U.S.A. 93*, 2285−2289.

BI981286B